

Joseph D. Adams, Terry L. Herter, George E. Gull, Justin Schoenwald, Charles P. Henderson, Luke D. Keller, James M. De Buizer, Gordon J. Stacey and Thomas Nikola, "FORCAST: a first light facility instrument for SOFIA", Proc. SPIE 7735, 77351U (2010).

Copyright 2010 Society of Photo Optical Instrumentation Engineers. One print or electronic copy may be made for personal use only. Systematic electronic or print reproduction and distribution, duplication of any material in this paper for a fee or for commercial purposes, or modification of the content of the paper are prohibited.

<http://dx.doi.org/10.1117/12.857049>

FORCAST: A “First Light” Facility Instrument for SOFIA

Joseph D. Adams^a, Terry L. Herter^a, George E. Gull^a, Justin Schoenwald^a, Charles P. Henderson^a,
Luke D. Keller^b, James M. De Buizer^c, Gordon J. Stacy^a, Thomas Nikola^a

^aDepartment of Astronomy, Space Sciences Building,
Cornell University, Ithaca, NY 14853-6801;

^bDepartment of Physics, Center for Natural Sciences, Ithaca College, Ithaca, NY 14850

^cUniversity Space Research Association, NASA Ames Research Center, Building N211, Moffett
Field, CA 94035-0001

ABSTRACT

FORCAST is the “first light” U. S. science instrument to fly aboard SOFIA. FORCAST offers dual channel imaging in discrete filters at 5 - 25 microns and 30 - 40 microns, with diffraction-limited imaging at wavelengths > 15 microns. FORCAST has a plate scale of 0.75 arcsec per pixel, giving it a 3.2 arcmin x 3.2 arcmin FOV on SOFIA. We give a status update on FORCAST development, including the performance of new far-IR filters; design and performance of the calibration box; laboratory operations and performance; and results from ground-based and first flight operations.

Keywords: Infrared cameras, blocked impurity band detectors, metal mesh filters

1. INTRODUCTION

The **F**aint **O**bject **i**nfra**R**ed **C**AMERA for the **S**ofia **T**elescope (FORCAST) is a dual-channel, wide-field camera designed to perform imaging in the infrared from 5-40 μm . FORCAST will be a facility instrument on the **S**tratospheric **O**bservatory **F**or **I**nfrared **A**stronomy (SOFIA). Our focus in this paper is to report recent laboratory test results, anticipated performance for the SOFIA early science phase, and limited results from the SOFIA telescope characterization and “first light” flight. We begin with a very brief description of FORCAST; for a more detailed description of the instrument design, see Keller *et al.* (2002)¹, Keller *et al.* (2004)², and Adams *et al.* (2006)³.

FORCAST is a cryogenic (4 K, with a 77 K shield) camera. Table 1 summarizes the FORCAST operational parameters. We use two detector arrays, a Si:As blocked impurity band (BIB) array for $\lambda < 25\mu\text{m}$ and a Si:Sb BIB array for $\lambda > 25\mu\text{m}$. Herter *et al.* (1998)⁴ present a review of BIB detectors for astronomy. Each of the detector array pixels maps to 0.75" on the sky and the total field-of-view is 3.2' square. Using two cameras allows simultaneous imaging in two bands (11-25 μm and 25-40 μm) with a cold dichroic beamsplitter splitting the telescope beam to the long wavelength channel (LWC) and the short wavelength channel (SWC). Our design enables high efficiency observations and takes advantage of the increased performance, relative to Si:Sb, of the Si:As BIB array for $\lambda < 25 \mu\text{m}$. With the Si:As BIB array, shorter wavelength (5-13 μm) imaging is possible by sliding the dichroic out of the beam and sliding a mirror into the beam, thereby directing the beam into the SWC. The LWC can also be used as a standalone camera by sliding the dichroic and mirror out of the beam and letting the beam be folded into the LWC camera. FORCAST allows selection of the bandpass independently for each channel via filter wheels. The selection of FORCAST filters for early science was made by the FORCAST team with input from the SOFIA science community. The filter suite covers several PAH features as well as continuum features (Table 2).

FORCAST is equipped with a pupil viewer in each channel consisting of a lens that images the Lyot stop onto the detector. The pupil viewers were used to align the FORCAST collimator mirror with the secondary mirror of the telescope. Additionally, the pupil viewers will be used to measure the emissivity of the telescope by providing the ability to measure sky emission that bypasses the telescope and reflects off the SOFIA tertiary mirror into FORCAST.

Table 1. FORCAST at a glance. All values are based on design or our laboratory test measurements.

Specification	SWC	LWC	Units
Detector Type	Si:As	Si:Sb	
Wavelength Range	5 - 25	25 - 40	μm
Well Size (Low Capacitance)	1.9×10^6	1.9×10^6	Electrons
Well Size (High Capacitance)	1.8×10^7	1.8×10^7	Electrons
Pixel width (square pixels)	50	50	μms
Field of View/Pixel	0.75	0.75	Arcseconds
Array Size	256x256	256x256	Pixels
Field of View/Array	3.2	3.2	Arcminutes
Average Optical Efficiency	30	30	%
Maximum Focal Plane Distortion	1.1	1.1	%
Array active area filling factor	> 95	> 95	%

Table 2. FORCAST filter set for SOFIA early science. Numbers in parenthesis are resolving power, $R=\lambda/\Delta\lambda$. ND represents neutral density filters. PAH filters include 6.3 μm , 7.7 μm , 8.6 μm , and 11.3 μm . The 11.1 μm , 19.7 μm , 24.2 μm , 31.4 μm , and 37.1 μm are used for continuum imaging. The 33.5 μm and 34.8 μm are designed to be order-blocking filters for future S [III] and Si [II] line Fabry-Perot filters. There are two grisms installed for spectroscopy; Grism 5 covers 17.1 μm – 28.1 μm , while Grism 6 covers 28.6 μm – 37.4 μm . The 11.8 μm filter is installed in the LWC for ground-based testing (the QE of the Si:Sb detector array extends down to 5 microns, but the Si:As detector has higher QE below $\sim 25 \mu\text{m}$).

Position	Filter Wheel			
	SWC 1	SWC 2	LWC 1	LWC 2
1	OPEN	24.2 μm (7.5)	37.1 μm (8.8)	Open
2	5.4 μm (33)	19.7 μm (3.8)	34.8 μm (8.3)	31.4 μm (5.7)
3	6.3 μm (48)	8.6 μm (42)	33.5 μm (17)	Grism 5 (140)
4	6.6 μm (34)	11.1 μm (12)	ND	11.8 μm (16)
5	7.7 μm (15)	11.3 μm (56)	Door Vignetting Test Mask	Door Vignetting Test Mask
6	ND	OPEN	OPEN	Grism 6 (250)

We have developed a sensitivity model to calculate the expected point source sensitivity of FORCAST in-flight. The model includes the transmission and thermal emission of the atmosphere; telescope emission and image quality; and the measured (when possible) or expected performance of the optics and detectors. Atmospheric transmission was determined using ATRAN software⁵. We measured the filter transmission curves at room temperature using a Fourier Transform Spectrometer. Quantum efficiency curves of Process Evaluation Chips were measured by the detector vendor (DRS Technologies, Anaheim, CA) and scaled to the quantum efficiency measured at Cornell for a bandpass filter⁶. Table 3 shows the typical assumptions and performance values used to compute the point source sensitivity. Table 4 lists the minimum detectable continuum flux (MDCF) for the filters in Table 2 necessary to achieve a signal-to-noise ratio of 4 in 900 seconds of integration time. Also listed in Table 4 are the center and pivot wavelengths⁷ that are computed from our laboratory measured filter transmission curves.

A suite of grisms has been developed under a separately funded and managed project to enable spectroscopy with FORCAST. The grisms cover most of the wavelengths accessible with FORCAST, at low to moderate resolution (140 – 1200). The grism modes are not currently supported as facility modes and will not officially be available for early science flights. However, two grisms are installed in the LWC in anticipation of future use. For details regarding the FORCAST grisms, see Ennico *et al.* (2006)⁸, Ennico *et al.* (2007)⁹, and Deen *et al.* (2008)¹⁰.

Table 3. Typical parameters used for the point source sensitivity model.

Parameter	Value
Source temperature	300 K
Altitude	41,000 ft.
Sky temperature	240 K
Water vapor overburden	7.1 μm
Primary mirror diameter	2.5 m
Elevation angle	40°
Telescope temperature	240 K
Telescope emissivity (estimated)	10%
Image quality (80% encircled energy)	5.3"
Window transmission	88%
Window temperature (estimated)	290 K
Reflectivity per FORCAST internal mirror	97%
Dichroic reflectivity (20 μm)	94%
Dichroic transmission (~30 – 40 μm)	42%
Filter transmission	See text
Read noise ⁹	2400 e- (high capacitance) 245 e- (low capacitance)
Quantum efficiency	See text
Pixel size	50 μm
Excess noise (βG) ⁴	2.5

Table 4. Minimum Detectable Continuum Flux (MDCF) for the model parameters given in Table 3, corresponding to a signal-to-noise ratio of 4 in 900 seconds of integration time. The center and pivot wavelengths⁷ were computed from our measured filter transmission curves (measured at room temperature).

Filter Name	Center (average) wavelength (μm)	Pivot Wavelength (μm)	Bandwidth (μm)	Resolving Power	MDCF (single channel) (mJy)	MDCF (dual channel) (mJy)
5.4	5.356	5.356	0.162	33	28.3	-
6.3	6.352	6.352	0.141	48	60.2	-
6.6	6.611	6.611	0.243	34	66.4	-
7.7	7.705	7.703	0.465	15	57.4	-
8.6	8.609	8.609	0.207	42	69.0	-
11.1	11.089	11.085	0.954	12	54.6	53.0
11.3	11.344	11.344	0.239	56	120	128
19.7	19.712	19.655	5.506	3.8	55.1	58.5
24.2	24.236	24.202	2.901	7.5	84.2	89.5
31.4	31.456	31.393	5.658	5.7	140	197
33.5	33.597	33.581	1.927	17.6	231	356
34.8	34.807	34.767	3.759	8.3	161	227
37.1	37.144	37.110	3.284	8.8	199	307

2. PERFORMANCE OF NEW METAL MESH FILTERS

We have augmented the filter suite described in Adams *et al.* (2008)¹¹ with several metal mesh filters (24.2 μm , 33.5 μm , 34.8 μm , and 37.1 μm). These filters were fabricated by Lakeshore Cryotronics, Inc. The 24.2 μm and 37.1 μm are

designed to be continuum imaging filters. The 33.5 μm and 34.8 μm filters were designed to be order-blocking filters for future [S III] and [Si II] line Fabry-Perot filters. However, they can be used standalone for continuum imaging as well. Figure 1 shows the transmission curves for the mesh filter configurations and an overlay of the atmospheric transmission at 41,000 feet altitude and 7.1 μm of water vapor burden overhead. Each filter configuration is a stack of two similar filters to improve out-of-band rejection compared with a single mesh filter. Note that the 37.1 μm transmits at wavelengths longer than 40 μm , but the Si:Sb detector QE falls off steeply above $\sim 40 \mu\text{m}$.

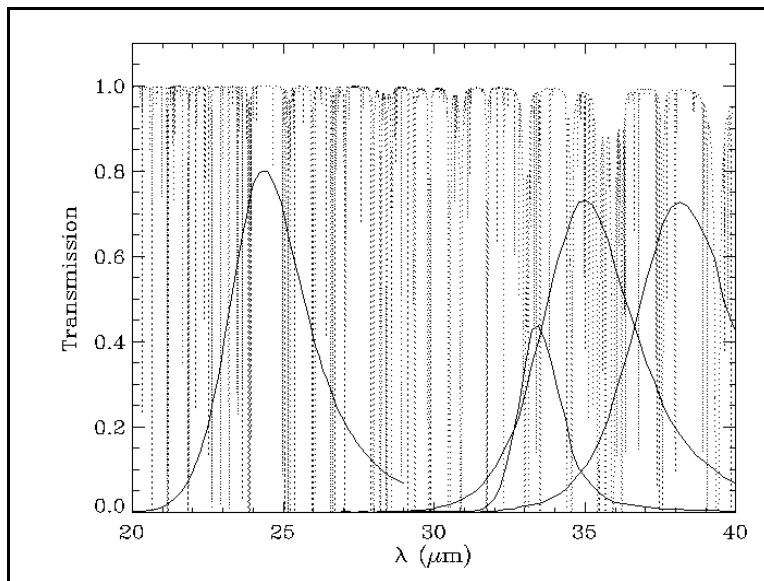


Figure 1. Filter transmission vs. wavelength λ for Lakeshore metal mesh filters centered near 24.2 μm , 33.5 μm , 34.8 μm , and 37.1 μm . Each filter transmission was measured using a Nicolet FTIR spectrometer. The filter curves correspond to a double stack (large gap) of two mesh filters with very similar center wavelengths and bandwidths. The QE of the Si:As detector is zero above $\sim 28 \mu\text{m}$, while the QE of the Si:Sb detector is zero above $\sim 40 \mu\text{m}$. The dotted line represents the atmospheric transmission at 41,000 feet altitude, 7.1 μm water vapor overburden, and 50° zenith angle.

3. CALIBRATION BOX DESIGN AND PERFORMANCE

FORCAST is equipped with a calibration box that is used to generate flat fields. The box is fixed to the FORCAST mounting plate just below the window and extends into the SOFIA Nasmyth tube when FORCAST is installed. A Peltier thermo-electric heater serves as a flux source. This source is imaged to the FORCAST pupil using a plano-convex, KRS-5 lens. An O-ring in the lens mount provides a pressure seal between the box volume and the Nasmyth tube. The source and lens are located below the FORCAST window, and their resulting optical beam is folded with a motorized, flat mirror into the FORCAST window. During normal telescopic observations, this flip mirror is rotated down with a stepper motor to cover the calibration box lens and allow FORCAST to view the telescope.

A commercial chopper blade slides in front of the source and is used to provide a reference for background subtraction. The position of the blade is controlled by a TTL signal from the FORCAST electronics to the chopper driver.

The temperature of the Peltier source is set from the FORCAST control PC through a serial link to the Peltier controller. Typically, $\Delta T = 20^\circ \text{C}$ between the reference and the source. This temperature differential results in a large signal ($S/N > 100$) on the FORCAST detectors at the nominal operating pixel well depth.

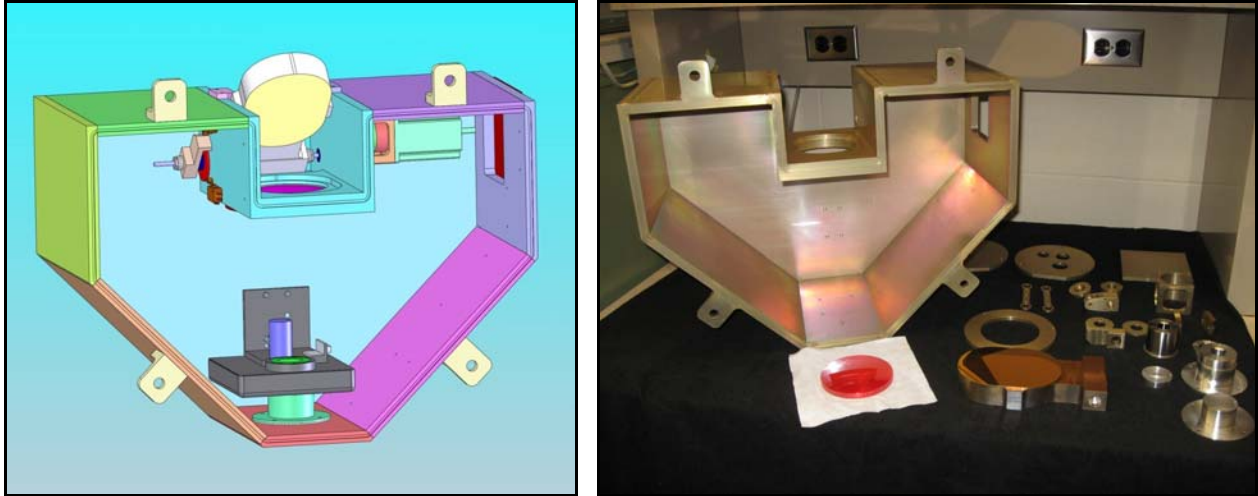


Figure 2. Calibration box design (left) and optical and mechanical components. A Peltier thermo-electric heater serves as a thermal flux source for FORCAST. A plano-convex KRS-5 lens images the source onto the FORCAST pupil. A commercial chopper blade acts as a reference for background subtraction. Finally, a flip mirror rotates to pick off the calibration beam into the FORCAST window, and rotates out of the telescope beam to “close” the calibration box during normal observations.

4. PRE-INSTALL LABORATORY TESTING

FORCAST is equipped with a set of external removable foreoptics (Figure 3) for laboratory testing and to couple FORCAST to the Palomar 200-inch telescope cassegrain focus. The foreoptics assembly is used to test data acquisition in stare, chopping, and nodding modes; for detector bias optimization; and to provide a rudimentary flux calibration which allows the calculation of in-flight performance estimates. The foreoptics assembly contains a thermal source, an object plane with a pinhole mask, a fast steering mirror at a pupil plane used for chopping, a shutter at the object plane to allow “nodding” (subtraction of the background thermal signature due to chopping). Two commercial gold-coated spherical mirrors and a convex mirror (a gold-coated lens) at the fast steering mechanism make up a modified Offner system. This system provides one-to-one imaging of the foreoptics’ object plane to the SOFIA focal plane internal to FORCAST and one-to-one imaging of the foreoptics’ pupil to the FORCAST Lyot stop. The focal pinhole plane mask contains several $457\ \mu\text{m}$ diameter pinholes that act as quasi-point sources, and one $1.6\ \text{mm}$ diameter pinhole that acts as an extended source. The thermal source is an electric Peltier cooler with bi-directional closed-loop temperature control that is stable to $< 0.01^\circ\ \text{C}$. Typical ΔT values between the mask and the thermal source (both are at unit emissivity) are $1^\circ\ \text{C}$ for SWC configurations and $2^\circ\ \text{C}$ for LWC configurations, for a signal-to-noise ratio of ~ 30 in 5 seconds of integration time (chop and nod subtraction). The fast steering mirror is a commercial two-axis steering mechanism composed of acoustic coils. A convex gold-coated lens comprises the mirror on the fast steering mechanism, also at the Offner pupil, which allows chopping. The FORCAST electronics generate a TTL signal used by the fast steering mirror drive electronics for chopping between 2 beams. The “nod” shutter is driven by a solenoid and slides between the thermal source and the focal plane mask to allow imaging of the focal plane and mirror emission for appropriate “nod” subtraction. The FORCAST electronics generate a second TTL signal that is accepted by the solenoid control and drive electronics for inserting or removing the nod shutter (also unit emissivity) from the foreoptics’ object plane.

Figure 4 shows an example of images taken with the foreoptics at $24.2\ \mu\text{m}$ and $37.1\ \mu\text{m}$. In addition to testing data acquisition in various modes, we perform photometry on the point sources to optimize the performance of the detector. Several detector parameters are varied to improve signal-to-noise. These parameters include detector bias voltage, pixel capacitance, and well depth. While increasing the detector bias improves responsivity, increased bias voltage can also worsen excess noise (larger βG), increase dark current exponentially, and increase the response of hot pixels that often cause a ringing noise in the multiplexer. Currently, we are running the arrays at $1.5\ \text{V}$ bias (SWC), $1.25\ \text{V}$ bias (LWC), low capacitance mode (whenever possible), and filling the wells to $\sim 2/3$ maximum well depth.

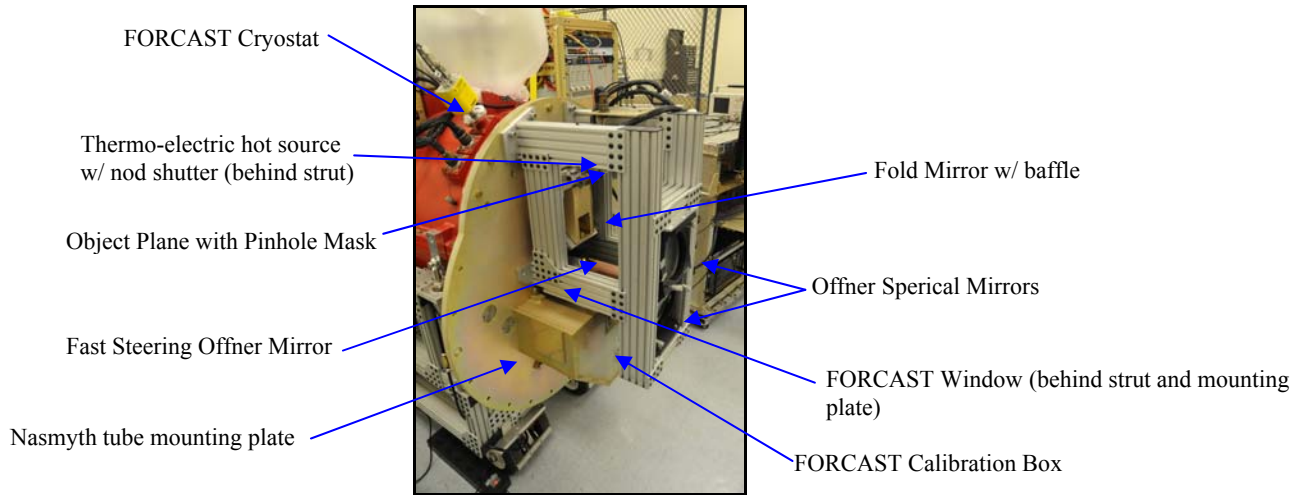


Figure 3. FORCAST foreoptics used for laboratory testing. Forcast is sideways-looking. The foreoptics contain an object plane with a pinhole mask and thermo-electric hot source. The foreoptics contain a modified Offner relay system with a fast steering mirror at the pupil, which is used to chop.

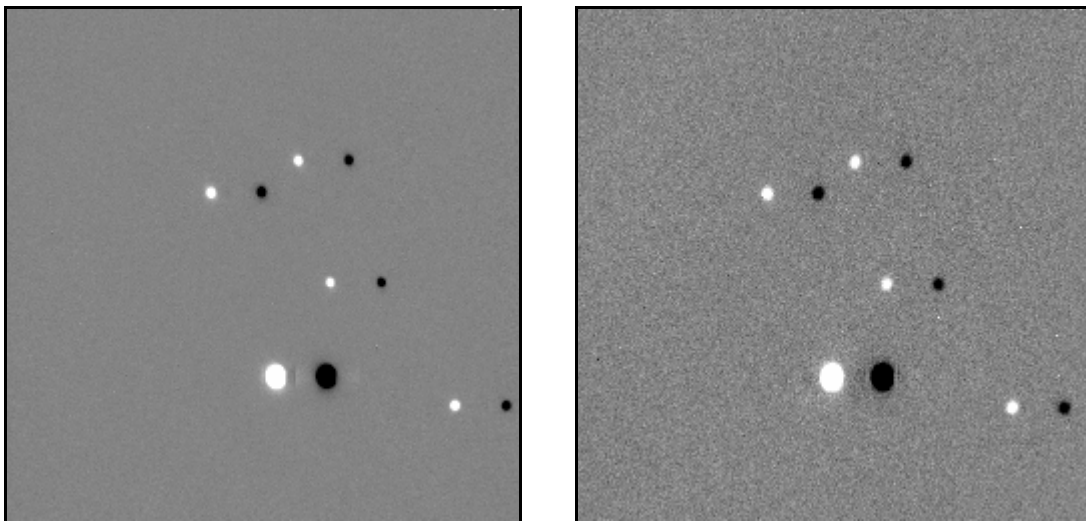


Figure 4. Chop and nod differenced images of “point” and “extended” sources (457 μm and 1.6 mm diameter pinholes) in the foreoptics at 24 μm (left) and 37 μm for $\Delta T = 5^\circ\text{C}$ and 5 sec integration time.

In order to measure telescope jitter and perform image motion compensation, FORCAST is capable of saving streamed images without coadding at high (~ 500 Hz) full frame rates. Approximately 4 Megapixels of 16-bit data are available to serve as storage for the data cubes. Subframes can be defined to increase the duration of the streaming data. For example, a 16×16 pixels subframe allows 16,384 frames to be stored in memory, corresponding to ~ 30 sec of streamed data at a full frame rate of 500 Hz. The detector multiplexer is incapable of operating in “burst” mode where only a subframe of the detector is clocked and read out. Rather, the full array is clocked and read out, but only the subframe is stored in memory.

In the lab, we use a serial interface-controlled function generator to drive the chop mirror with a low (< 100 Hz) signal that mimics telescope jitter. FORCAST can perform shift-and-add compensation for this jitter on-the-fly while coadding at ~ 500 Hz frame rate. The centroid of a point source is measured, and this information is used to align the images prior to coadding. During observations, we plan to use this mode on a star at 5 μm (where the star is most easily detected by

FORCAST), and use the motion in stellar position to compensate for the corresponding image motion in the LWC. Note the star must be detectable in a single read.

5. GROUND-BASED TESTING ON SOFIA

FORCAST was installed on SOFIA on May 7, 2010. Prior to first flight, several nights of ground testing occurred with SOFIA parked on the flight line. Ground testing included alignment of FORCAST to the telescope, focus testing, boresight determination, best chopper frequency and phase, a measurement of the telescope emissivity and chop and nod sequences for the in-flight science targets. The blank sky and a number of bright IR targets were used in the 8 – 13 μm atmospheric window, including Mars, α Boo, and μ Cep. Ground observations were performed using the 8.6 μm , 11.1 μm , 11.3 μm filters in the SWC and 11.8 μm filter in the LWC (the 11.8 μm filter was installed in the LWC specifically for ground-based testing). Additional ground tests will be performed before early science, including a test of an asymmetric chopping technique, and step-and-stare observations across a large science target (such as the Galactic Center or Orion Nebula).

Optical alignment to the telescope was performed on blank sky using the FORCAST pupil viewer in the SWC at 8.6 μm and the FORCAST tip/tilt collimator mirror. An image of the secondary mirror assembly through the FORCAST pupil viewer after alignment is shown in Figure 5. While the collimator was adjusted slightly away from its nominal lab settings, it was not tipped enough to cause vignetting at the field stop (the field stop is oversized by ~ 16 pixels in each direction).

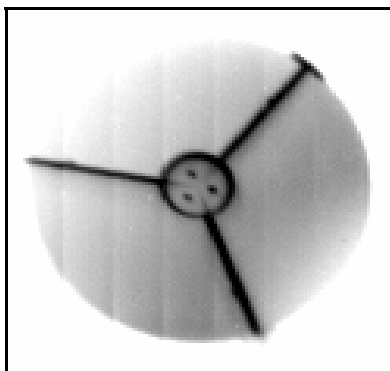


Figure 5. FORCAST image of the SOFIA telescope in front of blank sky taken in pupil viewer mode at 8.6 μm after alignment. The 3 dots near the center of the mirror are emission from the screwheads holding the reflective, conical secondary mirror button.

The center of the FORCAST field-of-view was determined to be aligned with the telescope boresight to within a few pixels. We determined that the position angle between the +Y direction in the FORCAST images and the positive telescope elevation direction was approximately 49° .

Using streamed data with fast (500 Hz) full frame rates in two-position chop mode on bright (> 500 Jy at 12 μm) sources, we measured the image quality on the ground at 8.6 μm and the secondary mirror chop settle time. The average FWHM was ~ 2 pixels. This includes the effects of system aberrations, seeing, and off-axis coma in the chopper. The measured image quality is consistent with achieving diffraction-limited performance at wavelengths > 15 μm . The chop settle time to achieve a FWHM within 1σ of the average settled FWHM was approximately 25 ms.

We also measured the telescope emissivity at 8.6 and 11 μm . In order to deconvolve the sky emission from the telescope emission, we measured the sky emission on the tarmac prior to installation, with FORCAST looking directly at the sky. Additionally, we were able to tip the collimator mirror to bypass the primary and secondary emission and view the sky directly via the SOFIA tertiary mirror. Figure 6 shows the pupil view of the sky with the collimator deliberately tipped to view the sky beyond the telescope. Finally, we measured the FORCAST CsI window (at room temperature) emissivity in the lab using a 77 K background. The window emissivity is $\sim 6\%$. We are currently analyzing the data from the telescope emissivity tests.

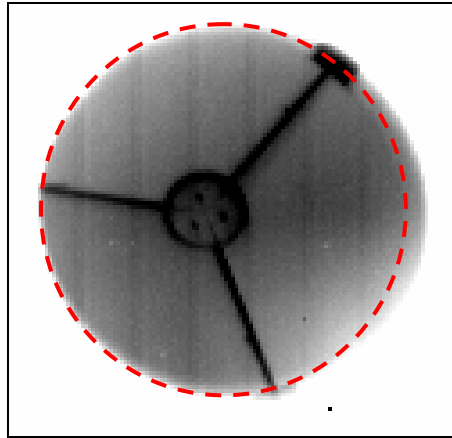


Figure 6. Pupil view of the sky at $8.6 \mu\text{m}$ with the FORCAST collimator mirror deliberately tipped to view the sky directly with the SOFIA tertiary mirror. The dashed line denotes the portion of the image corresponding to the telescope; outside this boundary FORCAST viewed the sky directly off the SOFIA tertiary mirror. A measurement of the sky emissivity is required for a measurement of the telescope emissivity.

6. TELESCOPE CHARACTERIZATION AND FIRST LIGHT FLIGHT

SOFIA first flight with a science instrument occurred with FORCAST on May 25, 2010. The goals of the flight were to characterize and optimize the telescope pointing stability and secondary mirror chopper performance under wind load, as well as demonstrate the scientific capability of the observatory. In-flight targets included α Sco, ϵ Sco, M82, and Jupiter, and several other IR stars.

For the telescope jitter measurements, FORCAST acquired data on the stars at $5.4 \mu\text{m}$ using the streamed data mode. Using a FORCAST subframe centered on a star, runs of ~ 20 sec at 500 Hz frame rate were taken to measure telescope jitter both with and without Flexible Body Compensation (FBC). In addition, tests of the chopper under wind load were performed using streamed data mode in runs up to 5 sec and $3'$ chop throw. Finally, the time-averaged jitter was measured while the FBC parameters were tuned. Results of the telescope testing will be presented elsewhere.

Two flight legs were performed on non-stellar targets: M82 (Figure 7) and Jupiter (Figure 8). Both objects were observed at 19.7 , 24.2 , 31.4 , and $37.1 \mu\text{m}$; additionally, Jupiter was imaged at $5.4 \mu\text{m}$. Chopping and nodding were performed on chip, with the chop direction in the cross-elevation direction and chop and nod amplitudes approximately $1' - 1.5'$. The nod direction was chosen in elevation for Jupiter and cross-elevation for M82. The infrared emission from M82 comes primarily from warm dust associated with star formation. The far-IR emission from Jupiter comes from the warm interior of Jupiter itself, except at $5.4 \mu\text{m}$ where a component of the infrared flux comes from reflected sunlight.



Figure 7. M82 at $19.7 \mu\text{m}$ (blue), $24.2 \mu\text{m}$ (green) and $37.1 \mu\text{m}$ (red). The scale of the image is approximately $1.5'$ in length. The infrared emission from M82 comes primarily from warm dust associated with star formation.



Figure 8. SOFIA First Light Infrared Images of Jupiter with Europa, Ganymede and Io at 5.4 μm (blue), 24.2 μm (green), and 37.1 μm (red). The IR images of Jupiter were deconvolved with a scaled Airy point spread function.

We have used Ganymede as a flux calibrator based on ISO spectral measurements published by Coustenis *et al.* (2002)¹². The flux is uncertain by 50% at 30 – 40 μm due to a discrepancy between the SWS and LWS channels. Nonetheless, our signal-to-noise is within a factor of 2 of our sensitivity predictions using an ATRAN atmosphere transmission corresponding to 35,000 feet altitude, 26.7 μm water vapor overburden, and 23° elevation angle. Note that there are other uncertainties with the calculation, namely the telescope emissivity and in-flight temperature of the FORCAST window. A more robust estimation of FORCAST sensitivities will be performed using observations of standard stars during early science flights and commissioning flights.

7. CONCLUSION

Based on its performance during lab, ground, and first flight tests, FORCAST is ready to embark on the SOFIA early science flights. Early Short Science consists of 3 flights with an emphasis on the Galactic Center and the Orion Nebula, and is scheduled for fall 2010. Early Basic Science consists of 12 science flights and is available to the general community. Proposal information for Basic Science is available at http://www.sofia.usra.edu/Science/proposals/basic_science/.

ACKNOWLEDGMENTS

FORCAST is supported by a grant from NASA administered by the Universities Space Research Association (USRA). SOFIA is operated by USRA.

REFERENCES

- [1] Keller, L. D., Herter, T. L., Stacey, G. J., Gull, G. E., Pirger, B., Schoenwald, J. and Nikola, T., “FORCAST: A Facility 5-40 micron camera for SOFIA”, Proc. SPIE 4014, 86 (2002).
- [2] Keller, L. D., Herter, T., Stacey, G., Gull, G., Schoenwald, J., Pirger, B., Adams, J., Berthoud, M., and Nikola, T., “First test results from FORCAST: the facility mid-IR camera for SOFIA,” Proc. SPIE 5492, 1086 (2004).
- [3] Adams, J. D., Herter, T. L., Keller, L. D., Gull, G. E., Pirger, B., Schoenwald, J., Berthoud, M., Stacy, G. J., and Nikola, T., “FORCAST: the facility mid-IR camera for SOFIA,” Proc. SPIE 6269, 34 (2006).
- [4] Herter, T. L., Hayward, T. L., Houck, J. R., Seib, D. H., and Lin, W. N., “Mid and far-infrared focal plane arrays for astronomy”, Proc. SPIE 3354, 109 (1998).
- [5] Lord, S. D., NASA Technical Memorandum 103957 (1992).
- [6] Adams, J. D., Herter, T. L., Keller, L. D., Gull, G. E., Pirger, B., Schoenwald, J., and Berthoud, M., “Testing of mid-infrared detector arrays for FORCAST,” Proc. SPIE 5499, 442 (2004).

- [7] Tokunaga, A. and Vacca, W., "The Mauna Kea Observatories Near-Infrared Filter Set. III. Isophotal Wavelengths and Absolute Calibration," *PASP*, 117, 421 (2005).
- [8] Ennico, K. A., Keller, L. D., Mar, D. J., Herter, T. L., Jaffe, D. T., Adams, J. D., and Greene, T. P., "Grism performance for mid-IR (5 - 40 micron) spectroscopy," *Proc. SPIE* 6269, 57 (2006).
- [9] Ennico, K., Keller, L., Adams, J., Herter, T., Deen, C., Mar, D., Chitrakar, N., Jaffe, D., and Greene, T., "Grisms For FORCAST - A New Medium Resolution 5-40 Micron Spectroscopic Mode On SOFIA - Performance Testing," *BAAS*, 211, 1114 (2007).
- [10] Deen, C. P., Jaffe, D. T., Marsh, J. P., Mar, D. J., Ennico, K. A., Greene, T. P., Keller, L., Chitrakar, N., Adams, J. D., and Herter, T., "A Silicon and KRS-5 Grism Suite for FORCAST on SOFIA," *Proc. SPIE* 7014, 81 (2008).
- [11] Adams, J. D., Herter, T. L., Gull, G. E., Schoenwald, J., Keller, L. D., Berthoud, M., Stacey, G. J., and Nikola, T., "FORCAST: the first light instrument for SOFIA", *Proc. SPIE* 7014, 80 (2008).
- [12] Coustenis, A., Encrenaz, Th., Lellouch, E., Salama, A., Müller, Th., Burgdorf, M. J., Schmitt, B., Feuchtgruber, H., Schultz, B., Ott, S., de Graauw, Th., Griffin, M. J., and Kessler, M. F., "Observations of Planetary Satellites with ISO", *Adv. Space Res.*, 30, 1971 (2002).